ORIGINAL RESEARCH PAPER
Volume - 14 | Issue - 09 | September - 2025 | PRINT ISSN No. 2277 - 8179 | DOI : 10.36106/ijsr
INTERNATIONAL JOURNAL OF SCIENTIFIC RESEARCH

"DIAGNOSTIC ACCURACY OF MRI IN CHARACTERIZING SELLAR AND PARASELLAR LESIONS: CORRELATION WITH HISTOPATHOLOGY"

Radio-Diagnosis

Bojanapally Preethi	Senior Resident, Dept Of Radio Diagnosis, Apollo Hospitals, Hyderabad.
Peethamber Lokanandi	Assistant Professor, Dept Of Radiodiagnosis, Gitam Institute Of Medical Sciences And Research, Visakhapatnam, Andhra Pradesh.
Mohd Abdul Rawoof*	Assistant Professor, Department Of Radiodiagnosis, Apollo Institute Of Medical Sciences And Research, Apollo Health City Campus, Road No.92, Jubilee Hills, Hyderabad, Telangana 500090. *Corresponding Author
Arige Raj Bharath Naidu	Senior Resident, Dept Of Radiology, Ayaan Institute Of Medical Sciences , Hyderabad.
Rallabandi Suresh Kumar	Senior Consultant Radiologist, Dept Of Radiology, Medicover Hospital, HITEC City, Hyderabad.
P. Adipudi Renuka	Consultant Radiologist, Dept Of Radiology, Medicover Hospital, HITEC City, Hyderabad.
Karanam Poorna Sasank	DM-IR Resident, Dept Of Interventional Radiology, DR.DY Patil Medical College, Pune.

ABSTRACT

Introduction: Sellar and parasellar lesions may present with non-specific complaints such as headache, confusion, diminished vision etc. and similar imaging findings2, diagnosis is usually made or suggested by the findings of the imaging studies. MRI remains the primary imaging modality for evaluating pituitary lesions, mixed nodules and some cystic lesions are difficult to diagnose. In such lesions, FDG PET can be used to characterize.2 **Aim/Purpose:** To evaluate the diagnostic accuracy of MRI in characterizing sellar and parasellar lesions correlating with Histopathology **Material And Methods:** This prospective analytical study at Apollo hospitals included patients with suspected sellar or parasellar lesions who underwent contrast-enhanced MRI brain. Findings were correlated with histopathology from biopsy or postsurgical specimens to assess diagnostic accuracy. **Results:** A total of 35 patients were studied. Among 35 patients, MRI accurately diagnosed 33 cases (94.3%). Accuracy was 100% for pituitary macroadenoma, meningioma, and Rathke's cleft cyst, and 66.7% for craniopharyngioma. Two cases misdiagnosed as macroadenoma were later confirmed as craniopharyngioma. **Conclusion:** In the study, significant correlation was found between MRI and HPE findings.

KEYWORDS

Sellar and parasellar lesions, MRI, Histopathology

INTRODUCTION:

The skull base houses complex neurovascular structures, making sellar and parasellar lesions difficult to characterize, as diverse pathologies often present with similar imaging features.[1] Most sellar and parasellar lesions present with non-specific symptoms like headache, confusion, or visual disturbances, making imaging crucial for diagnosis. Pituitary tumors comprise ~15% of intracranial masses, ~90% being adenomas—most commonly prolactinomas, followed by nonfunctioning and GH-secreting adenomas. Other lesions include Rathke's cleft cysts (most common non-adenomatous mass), craniopharyngiomas, meningiomas, germ cell tumors, gliomas, lymphomas, metastases, and other cystic lesions.[3] In adults, pituitary adenomas are the most common pituitary disease, whereas in children, adenomas predominate but are followed more frequently by craniopharyngiomas and germ cell tumors.[4] Pituitary carcinomas are rare in adults and exceedingly rare in children. Symptoms vary with lesion type, hypothalamic–pituitary or visual pathway involvement, and cavernous sinus extension, presenting as endocrine, neurological, or ophthalmological manifestations. Incidental lesions are also noted, with a prevalence of ~9.3% in autopsy series and 0.1–0.3% on MRI.[5] Most of the pituitary adenomas are detected incidentally on routine CT imaging.[6] Extra-axial tumors are the most common group, typically slow-growing and insidious, but early detection is crucial as surgical resection can preserve function. Accurate diagnosis requires understanding their classification, pathology, imaging features, and differentials by location. In children, MRI is the modality of choice, relying on detailed knowledge of anatomy and normal signal characteristics.[7]

The advances that have occurred in the imaging modalities of the brain provide extensive detail of anatomic relationships and have led to an increased detection rate of sellar and parasellar masses.

Role Of Imaging In Sellar And Parasellar Lesions:

Imaging of sellar and parasellar lesions has progressed from skull radiographs to CT and MRI. While CT is useful for detecting calcifications and bone erosion, MRI is safer and superior for assessing tumor extent and involvement of adjacent structures. The SIPAP MRI classification of pituitary adenomas—based on parasellar, suprasellar, infrasellar, anterior, and posterior extension—provides a simple, reliable tool for preoperative planning and minimizing surgical complications.[8] MRI also helps localize the optic pathways in sellar and parasellar tumors, aiding preoperative planning and surgical approach selection.[9] While MRI is the primary tool for pituitary evaluation, mixed nodules and certain cystic lesions may be difficult to characterize, where FDG PET can provide additional value.[2]

Rationale And Purpose Of The Study:

This prospective study assessed the diagnostic accuracy of MRI in characterizing sellar and parasellar lesions using histopathology as the gold standard, with analysis of imaging patterns and lesion distribution by age and sex to enhance diagnostic precision and patient management.

Study Definitions:

SIPAP MRI Classification Of Pituitary Adenomas:

- **Suprasellar (5 Grades):** 0 – none; 1 – bulge not reaching chiasm; 2 – reaching chiasm without displacement; 3 – displacing chiasm; 4 – causing hydrocephalus.
- **Infrasellar (3 Grades):** 0 – none; 1 – focal bulge with dural/floor perforation; 2 – extension into sphenoid sinus.
- **Parasellar (5 Grades):** 0 – medial to ICA; 1 – up to intercarotid line; 2 – up to lateral tangent; 3 – beyond lateral tangent; 4 – encasing ICA bilaterally.
- **Anterior (2 Grades):** 0 – none; 1 – extension into anterior cranial

fossa.

- **Posterior (3 Grades):** 0 – none; 1 – posterior superior growth; 2 – posterior inferior growth.

MATERIAL AND METHODS:

This prospective analytical study was conducted in the Dept of Radiodiagnosis, Apollo Hospitals, Hyderabad, over two years (March 2022–Feb 2024). Patients with suspected sellar or parasellar lesions underwent contrast-enhanced MRI, and findings were correlated with histopathology (biopsy or postsurgical) to determine diagnostic accuracy.

Inclusion: Patients undergoing brain MRI with suspected sellar/parasellar lesions.

Exclusion: Pregnant/lactating women, renal impairment, MRI-incompatible implants/foreign bodies, or claustrophobia.

Study Imaging Procedure:

A total of 35 patients with MRI-diagnosed sellar or parasellar lesions were followed up with biopsy or surgical excision findings for confirmation.

MRI protocol included axial, sagittal, and coronal scans from the anterior skull base to posterior brainstem. Sequences obtained were high-resolution sagittal T1, coronal T1, and coronal T2. All patients received gadolinium-based contrast (0.1 mmol/kg; ~10 mL at 3 mL/sec), followed by post-contrast T1 images in all planes. In suspected microadenomas, dynamic coronal T1 imaging was performed with divided contrast dosing and acquisition over 2.5 minutes.

Study Outcomes:

MRI diagnoses based on lesion features, extent, adjacent relations, and vascular involvement were correlated with histopathology; indeterminate cases were finalized as benign or malignant with histopathologist review.

Study Statistical Analysis Plan:

The Chi-square test was used to assess the association between MRI and histopathological diagnoses. Diagnostic accuracy of MRI was calculated using histopathology as the gold standard. Data were entered in MS Office and analyzed with SPSS v19. A p-value <0.05 was considered statistically significant, and results were presented with relevant graphs.

RESULTS:

Out of 35 patients, 4 (11.4%) were ≤14 years old; 18 (51.4%) were female and 17 (48.6%) were male.

Table 1: Age Distribution Versus Histopathology.

Age (Years)	Histopathology				Total
	Craniopharyngioma	Meningioma	Pituitary macroadenoma	Rathke's cleft cyst	
<=14	4(66.7%)	0	0	0	4(11.4%)
15 & Above	2(33.3%)	3 (100%)	23(100%)	3(100%)	31(88.6%)
Total	6	3	23	3	35
p-value (Chi-Square Test): <0.001					

Table 2: Gender Distribution Versus Histopathology

Sex	Histopathology				Total
	Craniopharyngioma	Meningioma	Pituitary macroadenoma	Rathke's cleft cyst	
Male	4(66.7%)	0	13(56.5%)	0	17
Female	2(33.3%)	3(100%)	10(43.4%)	3	18
Total	6	3	23	3	35
p-value (Chi-Square Test) = 0.05					

In this study, pituitary macroadenomas and meningiomas were predominantly isointense on T1, while craniopharyngioma and Rathke's cleft cysts were mainly hypointense, with a significant association (p = 0.004).

Table 3: T1 Characteristics Of Lesions Versus Histopathology.

MRI T1	Histopathology				Total
	Craniopharyngioma	Meningioma	Pituitary macroadenoma	Rathke's cleft cyst	
Hyper	0 (0 %)	0 (0 %)	4 (17.4 %)	1 (33.3 %)	5
Iso	2 (33.3 %)	3 (100 %)	10 (43.5 %)	0 (0 %)	15
Hypo	4 (66.7 %)	0 (0 %)	9 (39.1 %)	2 (66.7 %)	15
Total	6	3	23	3	35
p-value (Chi-Square Test) = 0.004					

Pituitary macroadenomas and Rathke's cleft cysts were commonly hyperintense on T2, while craniopharyngiomas and meningiomas were exclusively hyperintense, with a significant association (p = 0.028).

Table 4: T2 Characteristics Of Lesions Versus Histopathology.

MRI T2	Histopathology				Total
	Craniopharyngioma	Meningioma	Pituitary macroadenoma	Rathke's cleft cyst	
Hetero	0 (0 %)	0 (0 %)	2 (8.7 %)	0 (0 %)	2
Hyper	6 (100 %)	3 (100 %)	16 (69.6 %)	2 (66.7 %)	25
Hypo	0 (0 %)	0 (0 %)	5 (21.7 %)	1 (33.3 %)	8
Total	6	3	23	3	35
p-value (Chi-Square Test) = 0.028					

Only 3 pituitary macroadenomas (13.0%) showed diffusion restriction, while other lesions did not; the association between DWI/ADC characteristics and histopathology was not significant (p = 0.634).

Table 5: DWI/ADC Characteristics Of Lesions Versus Histopathology.

MRI DWI/ADC	Histopathology				Total
	Craniopharyngioma	Meningioma	Pituitary macroadenoma	Rathke's cleft cyst	
Yes	0 (0 %)	0 (0 %)	3 (13 %)	0 (0 %)	3
No	6 (100 %)	3 (100 %)	20 (87 %)	3 (100 %)	32
Total	6	3	23	3	35
p-value (Chi-Square Test) = 0.634					

All craniopharyngiomas and Rathke's cleft cysts had a cystic component, seen in 21.7% of pituitary macroadenomas but absent in meningiomas, with a significant association (p = 0.013).

Table 6: Presence Of Cystic Component In Lesions Versus Histopathology.

MRI Cystic component	Histopathology				Total
	Craniopharyngioma	Meningioma	Pituitary macroadenoma	Rathke's cleft cyst	
Yes	6 (100 %)	0 (0 %)	5 (21.7 %)	3 (100 %)	22
No	0 (0 %)	3 (100 %)	18(69.6 %)	0 (0 %)	13
Total	6	3	23	3	35
p-value (Chi-Square Test) = 0.013					

Blooming on SWI was seen in 83.3% of craniopharyngiomas, while most pituitary macroadenomas (69.6%) and all meningiomas and Rathke's cleft cysts showed none, with a significant association (p = 0.021).

Table 7: SWI Characteristics In Lesions Versus Histopathology.

MRI FFE	Histopathology				Total
	Craniopharyngioma	Meningioma	Pituitary macroadenoma	Rathke's cleft cyst	
Yes	5 (83.3 %)	0 (0 %)	7 (30.4 %)	0 (0 %)	12
No	1 (16.7 %)	3 (100 %)	16 (69.6 %)	3 (100 %)	23
Total	6	3	23	3	35
p-value (Chi-Square Test) = 0.021					

All pituitary macroadenomas and Rathke's cleft cysts were sellar in origin with suprasellar extension; most macroadenomas also showed parasellar spread. Craniopharyngiomas (4/6) were sellar with suprasellar extension, while all meningiomas (3/3) were suprasellar,

some extending anteriorly.

Table 8: Location And Extent Of Lesions Among The Study Population Versus Histopathology.

Location and Extension	Histopathology				P Value
	Craniopharyngioma	Meningioma	Pituitary macroadenoma	Rathke's cleft cyst	
Sellar	4	0	23	3	<0.001
Suprasellar origin	2	3	0	0	<0.001
Suprasellar Extension	4	0	20	3	<0.001
Parasellar Extension	0	0	16	0	0.002
Infrasellar Extension	0	0	3	0	0.634
Anterior Extension	0	2	4	0	0.071
Posterior Extension	2	0	3	0	0.422

Most pituitary macroadenomas showed Grade 2 suprasellar extension (34.8%), followed by Grade 1 (30.4%) and Grade 3 (30.4%). Parasellar extensions were evenly distributed between Grades 1 and 2, while few lesions showed Grade 1 infrasellar (13.0%), Grade 1 anterior (17.4%), and Grade 2 posterior (13.0%) extensions.

Table 9: MRI Extension Of Pituitary Macroadenoma Versus Histopathology.

	Grade 0	Grade 1	Grade 2	Grade 3	Grade 4
Suprasellar Extension	0	7	8	7	1
Parasellar Extension Right	8	7	6	2	1
Parasellar Extension Left	7	9	4	3	0
Infrasellar Extension	20	3	0	0	0
Anterior Extension	19	4	0	0	0
Posterior Extension	20	3	0	0	0

Heterogeneous enhancement was seen in 78.3% of pituitary macroadenomas and all craniopharyngiomas, while meningiomas enhanced homogeneously and Rathke's cleft cysts showed none, with a significant association ($p < 0.001$).

Table 10: Post-contrast Enhancement Characteristics In Lesions Versus Histopathology.

MRI P/C T1 Enhancement	Histopathology				Total
	Craniopharyngioma	Meningioma	Pituitary macroadenoma	Rathkes cleft cyst	
Heterogeneous	6 (100 %)	0 (0 %)	18 (78.3 %)	0 (0 %)	24
Homogeneous	0 (0 %)	3 (100 %)	5 (21.7 %)	0 (0 %)	8
No Enhancement	0 (0 %)	0 (0 %)	0 (0 %)	3 (100 %)	3
Total	6	3	23	3	35
p-value (Chi-Square Test) < 0.001					

Of 35 subjects, MRI diagnosed pituitary macroadenoma in 25, craniopharyngioma in 4, and Rathke's cleft cyst and meningioma in 3 each.

Table 11: Final Diagnosis On MRI Among The Study Population.

Histopathology	No. of Subjects	Percentage
Craniopharyngioma	6	17.1%
Meningioma	3	8.6%
Pituitary macroadenoma	23	65.7%
Rathke's cleft cyst	3	8.6%
Total	35	

On histopathology, 23 had pituitary macroadenoma, 6 craniopharyngioma, and 3each Rathke's cleft cyst and meningioma.

Table 12: Final Diagnosis On Histopathology Among The Study Population.

MRI Diagnosis	No. of Subjects	Percentage
Craniopharyngioma	4	11.4%
Meningioma	3	8.6%
Pituitary macroadenoma	25	71.4%
Rathke's cleft cyst	3	8.6%
Total	35	

MRI showed 100% accuracy for craniopharyngioma, meningioma, and Rathke's cleft cyst, while 23/25 pituitary macroadenomas were confirmed, with 2 mismatches; the association with histopathology was significant ($p < 0.001$).

Table 13: MRI Diagnosis Versus Histopathology Among The Study Population.

MRI Diagnosis	Histopathology				Total
	Craniopharyngioma	Meningioma	Pituitary macroadenoma	Rathke's cleft cyst	
Craniopharyngioma	4 (66.7 %)	0 (0 %)	0 (0 %)	0 (0 %)	4
Meningioma	0 (0 %)	3 (100 %)	0 (0 %)	0 (0 %)	3
Pituitary macroadenoma	2 (33.3 %)	0 (0 %)	23 (100 %)	0 (0 %)	25
Rathke's cleft cyst	0 (0 %)	0 (0 %)	0 (0 %)	3 (100 %)	3
Total	6	3	23	3	35
p-value (Chi-Square Test) < 0.001					

Most sellar and parasellar lesions showed MRI–histopathology concordance, with matching rates of 100% for pituitary macroadenoma, meningioma, and Rathke's cleft cyst, and 66.7% for craniopharyngioma; the association was significant ($p < 0.017$).

Table 14: MRI Matching Versus Histopathology Among The Study Population

MRI Matching	Histopathology				Total
	Craniopharyngioma	Meningioma	Pituitary macroadenoma	Rathke's cleft cyst	
Yes	4 (66.7 %)	3 (100 %)	23 (100 %)	3 (100 %)	33
No	2 (33.3 %)	0 (0 %)	0 (0 %)	0 (0 %)	2
Total	6	3	23	3	35
p-value (Chi-Square Test) = 0.017					

Illustrations:

Illustration -1

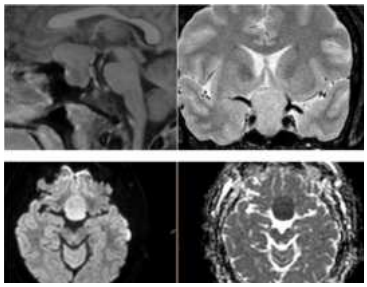

Figure 1: A 37-year-old male with visual symptoms had a sellar lesion (T1 isointense, T2 hyperintense, restricted diffusion, heterogeneous enhancement, no cyst/blooming) with suprasellar (G3), posterior (G2), anterior (G1), bilateral parasellar, and infrasellar extensions. MRI suggested pituitary macroadenoma, confirmed histologically.

Illustration -2

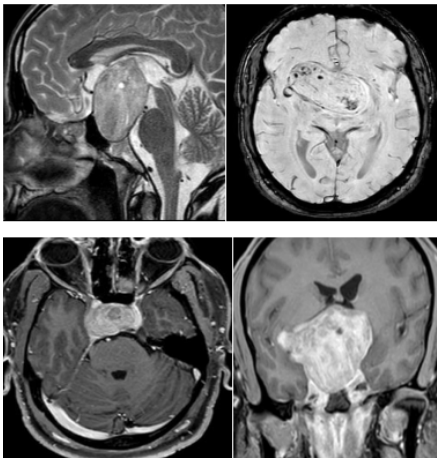

Figure 2: A 36-year-old male with headache and visual symptoms had a widened sella with a large T1 isointense, T2 heterogeneously hyperintense lesion showing heterogeneous enhancement, cystic/necrotic areas, and SWI blooming. Extensions: suprasellar (G5), right parasellar with ICA encasement (G4), left parasellar (G3), anterior/posterior/infrasellar (G1). MRI suggested pituitary macroadenoma, confirmed histologically.

Illustration -3

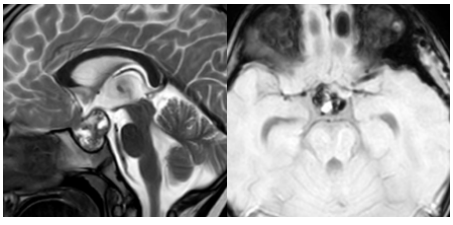

Figure 3: A 2-year-old girl had a 22×15 mm sellar–suprasellar lesion with heterogeneous T2 signal, SWI blooming, and optic chiasm abutment. MRI suggested craniopharyngioma, confirmed histologically.

Illustration - 4

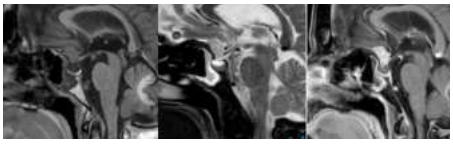

Figure 4: A 64-year-old female with headache had a suprasellar extra-axial lesion (T1 isointense, T2/FLAIR hyperintense) with homogeneous enhancement, dural tail, and tuberculum sella extension; pituitary separate. MRI suggested planum sphenoidale/ tuberculum sella meningioma, confirmed histologically.

Illustration 5

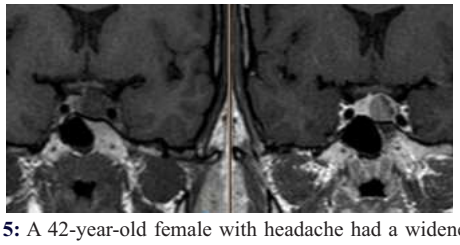

Figure 5: A 42-year-old female with headache had a widened sella with a left-sided T1 hypointense, T2 heterointense lesion showing heterogeneous hypoenhancement, Grade 1 left parasellar/suprasellar extension, normal right pituitary enhancement, and mild stalk deviation without blooming. MRI suggested pituitary macroadenoma, confirmed histologically.

Illustration 6

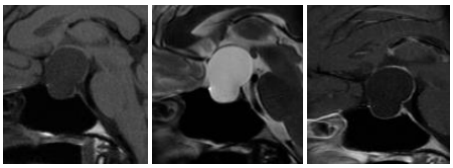

Figure 6: A 22-year-old female with headache had a sellar–suprasellar cystic lesion (T1 hypointense, T2 hyperintense, non-enhancing) abutting and displacing the optic chiasm. MRI suggested Rathke's cleft cyst, confirmed histologically.

DISCUSSION:

In our study, MRI accuracy for sellar and parasellar lesions was 94.3%. Diagnostic accuracy was 100% for pituitary macroadenoma, meningioma, and Rathke's cleft cyst, and 66.7% for craniopharyngioma. Two MRI-diagnosed macroadenomas were histopathologically confirmed as craniopharyngiomas.

In Pratisruti Hui et al.[10] MRI showed 94% overall accuracy, with lesion-specific accuracy of 94.1% for macroadenoma, 94% for craniopharyngioma, 100% for meningioma, glioma, and epidermoid, and 98% for germinoma. Misdiagnoses included one macroadenoma and one germinoma as craniopharyngioma, and one craniopharyngioma as macroadenoma. Our study showed similar overall accuracy, though with lower accuracy for craniopharyngioma.

In Suman Chaudhary et al.[11] MRI showed 94% overall accuracy, with lesion-specific accuracy of 100% for pituitary macroadenoma, meningioma, and schwannoma, and 75% for craniopharyngioma.

Table 15: Comparison Of Overall Accuracy Of The Study.

STUDY	OVERALL ACCURACY
Pratisruti Hui et al. [25]	94%
Suman chaudhary et al. [24]	94%
Our Study	94.3%

In our study, 88.6% were ≥15 years and 11.4% ≤14 years. Craniopharyngiomas showed bimodal distribution, while macroadenomas, meningiomas, and Rathke's cleft cysts predominated in older patients. Pratisruti Hui et al.[10] similarly reported most cases (58%) in the 20–49 age group. A secondary objective was to describe MRI features.

In our study, 23/35 patients had pituitary macroadenomas: 43.5% T1 isointense, 69.6% T2 hyperintense, mostly solid with few cystic, 30.4% with SWI blooming. They arose from the sella with suprasellar extension (G2: 34.8%, G1: 30.4%, G3: 30.4%), balanced parasellar spread, and occasional infrasellar (13%), anterior (17%), and posterior (13%) extensions. Enhancement was mainly heterogeneous (78.3%). Findings matched Suman Chaudhary et al.[11], with minor enhancement differences.

Among 35 patients, 6 had craniopharyngiomas; 66.7% were T1 hypointense, all T2 hyperintense, solid-cystic, with SWI blooming in 83.3% and no diffusion restriction. Most were sellar with suprasellar extension and showed heterogeneous enhancement. Findings matched Suman Chaudhary et al.[11] MRI correctly diagnosed 4/6, while 2 were misdiagnosed as macroadenomas.

Of 35 patients, 3 had meningiomas, all T1 isointense, T2 hyperintense, solid, without SWI blooming or diffusion restriction. They were mainly suprasellar with some anterior extension and showed homogeneous enhancement. Findings were consistent with Suman Chaudhary et al.[11]

Of 35 patients, 3 had Rathke's cleft cysts; 66.7% were T1 hypointense and T2 hyperintense. All were purely cystic, without blooming, diffusion restriction, or enhancement, and arose from the sella with suprasellar extension. Findings agreed with Kim G et al.[12].

Limitations:

Our 35-patient sample limited validity and disease spectrum assessment. Only surgically/biopsy-confirmed cases were included, excluding smaller asymptomatic lesions; longer duration may address this. Use of 1.5T MRI was another limitation, as 3T offers better resolution for sellar–parasellar evaluation.

CONCLUSIONS:

The study highlights a significant correlation between MRI and histopathology, supporting MRI as a reliable diagnostic modality for sellar and parasellar lesions.

Financial Support And Sponsorship: Nil.
Conflicts Of Interest: There are No conflicts of interest.

REFERENCES:

1. Zamora C, Castillo M. Sellar and parasellar imaging. Neurosurgery. 2017 Jan1;80 (1):17 -38.
2. Seok H, Lee EY, Choe EY, Yang WI, Kim JY et al. Analysis of 18Ffluorodeoxyglucose positron emission tomography findings in patients with pituitary lesions. The Korean journal of internal medicine. 2013 Jan;28(1):81.
3. Famini P, Maya MM, Melmed S. Pituitary magnetic resonance imaging for sellar and parasellar masses: ten-year experience in 2598 patients. The Journal of Clinical Endocrinology & Metabolism. 2011 Jun 1;96(6):1633-41.
4. Castellanos LE, Misra M, Smith TR, Laws ER, Iorgulescu JB. The epidemiology and management patterns of pediatric pituitary tumors in the United States. Pituitary. 2021 Jun;24:412-9.
5. Bresson D, Herman P, Polivka M, Froelich S. Sellar lesions/pathology. Otolaryngologic Clinics of North America. 2016 Feb 1;49(1):63-93.
6. Russ S, Anastasopoulou C, Shafiq I. Pituitary adenoma. InStatPearls [Internet] 2023 Mar 27. StatPearls Publishing.
7. Shields R, Mangla R, Almast J, Meyers S. Magnetic resonance imaging of sellar and juxtasellar abnormalities in the paediatric population: an imaging review. Insights into Imaging. 2015 Apr;6:241-60.
8. Anwar SS, Hilal K, Khan A, Ahmad A. Magnetic resonance imaging grading of pituitary macroadenoma–SIPAP classification revisited. European Journal of Radiology Open. 2023 Jan 1;10:100486
9. Saeki N, Murai H, Kubota M, Fujimoto N, Iuchi T et al. Heavily T2 Weighted MR Images of Anterior Optic Pathways in Patients with Sellar and Parasellar Tumours–rediction of Surgical Anatomy. Acta neurochirurgica. 2002 Jan;144:25-35.
10. Hui P, Parida S, Mohanty J, Singh M, Sarangi PK. Accuracy of magnetic resonance imaging in evaluation of sellar and juxtasellar tumors. Oncology Journal of India. 2019 Jan 1;3(1):3-9.
11. Dr. Suman Chaudhary, Dr. Anand Prakash Verma and Dr. Pankaj Gupta , 2019. "Role of MRI in Evaluation of Sellar, Parasellar and Suprasellar lesion with Histopathological Correlation", International Journal of Current research ,11, (08), 6084-6093.
12. Kim G, Moon JH, Kim SH, Kim EH. MRI-based classification of Rathke's cleft cyst and its clinical implication. Brain Tumor Res Treat. 2023 Jan 1;11:59-65.